Tetracyanoquinodimethanido Derivatives of (Terpyridine)- and (Phenanthroline)metal Complexes − Structural and Magnetic Studies of Radical-Ion Salts[‡]

Cristina Alonso,[a] Loreto Ballester,[a] Angel Gutiérrez,*[a] M. Felisa Perpiñán,[a] Ana E. Sánchez,[a] and M. Teresa Azcondo[b]

Keywords: Radical ions / Stacking interactions / Supramolecular chemistry / Magnetic properties

Several derivatives of formulae $[M(terpy)_2](TCNQ)_2$ or $[M(terpy)_2](TCNQ)_3$ (M = Ni, Cu, Zn; terpy = 2,2′:6′,2"-terpyridine; TCNQ= 7,7,8,8-tetracyanoquinodimethane) and $[M(phen)_3](TCNQ)_2$ or $[M(phen)_3](TCNQ)_4$ (M = Fe, Ni; phen = 1,10-phenanthroline) have been obtained. The crystal structures of $[M(terpy)_2](TCNQ)_2$ (M = Ni, Cu) show that the metal is surrounded by the terpyridine nitrogen atoms in a closed octahedral environment and the TCNQ anions are dimerised by π overlap. The cationic $[M(terpy)_2]^{2+}$ and the anionic $[TCNQ]_2^{2-}$ groups alternate in the crystal. For the derivatives with three TCNQ groups, the existence of a stack of trimeric $[TCNQ]_3^{2-}$ ions having electronic delocalisation is proposed. The compound $[Fe(phen)_3](TCNQ)_2$, which shows a strong interaction between TCNQ anions, led to the formation of a σ bond in the diamagnetic species [TCNQ–TCNQ], while the nickel analogue is expected to have a localised structure formed by alternation of cationic metal complexes and dimeric $[TCNQ]_2^{2-}$ anions similar to those observed in the analogous terpy derivatives. The derivatives having four TCNQ groups also show electronic delocalisation and a 1D stack based on the magnetic data is proposed.

Introduction

In the field of molecular networks containing organic radicals, macroscopic properties such as magnetic order or electric conductivity can be produced when the appropriate supramolecular arrangement is achieved.[1,2] On this basis, when paramagnetic metallic centres are integrated within organic radicals as building blocks in molecular networks, "hybrid" materials combining the properties of the organic and inorganic components can be formed.[3,4]

Special attention has been given to the assembly of organonitrile radical complexes with transition metals because of their rich interaction possibilities. One of the most extensively used radicals in these studies has been the planar organic molecule 7,7,8,8-tetracyanoquinodimethane (TCNQ) since it shows a low reduction potential which makes it a suitable acceptor in charge transfer processes and also shows, in its anion-radical form, a high σ-donor ability for coordinating to transition metals.[5−8] Another typical feature of this acceptor is the tendency to overlap its π-delocalised system with neighbouring molecules to form stacks with different degrees of electronic delocalisation.[9−12]

The compounds having vacant positions around the metal react with TCNQ salts forming new compounds where the anion-radical is coordinated via one or more of its nitrile groups.[6,8,13−15] When complexes with a fully coordinated metal environment are used, new species without direct bonding interactions between the metal and the TCNQ are formed. When TCNQ is fully reduced, dimerisation to $[TCNQ]_2^{2-}$ is usually observed[7,8,16] but when TCNQ is partially reduced, a greater electronic delocalisation along with the formation of infinite stacks is observed.[9−12]

The present work reports our studies on the interactions of TCNQ in different formal oxidation states with closed shell first row transition metal complexes aimed at looking for electronic delocalisation in our systems. We have used nitrogen donor ligands with aromatic rings such as terpy (2,2′:6′,2"-terpyridine) or phen (1,10-phenanthroline) which are susceptible to forming weak π interactions with the TCNQ rings.[17−26] These interactions are more common when neutral TCNQ is present and can modulate the TCNQ overlap responsible for the stacking.

[‡] A portion of this work was previously published in communication form: L. Ballester, A. Gutiérrez, M. F. Perpiñán, M. T. Azcondo, A. E. Sánchez, *Synth. Met.* **2001**, *120*, 965.

[a] Departamento de Química Inorgánica I, Facultad de Ciencias Químicas, Universidad Complutense,
28040 Madrid, Spain
Fax: (internat.) + 34-913944352
E-mail: alonso@quim.ucm.es
[b] Departamento de Ciencias Químicas, Facultad de Ciencias Experimentales y de la Salud, Universidad San Pablo, CEU,
28668 Boadilla del Monte, Madrid, Spain

  DOI: 10.1002/ejic.200400540

Results and Discussion

All metallic compounds were obtained by metathesis reactions from the parent derivatives. When only anionic TCNQ was added to the reaction mixture in the form of LiTCNQ, the compounds $[M(terpy)_2](TCNQ)_2$, (M = Ni, **1**; Cu **2**; Zn, **3**) or $[M(phen)_3](TCNQ)_2$, (M = Fe, **7**, Ni **8**) were obtained. TCNQ is in the anionic form in each case since it must neutralise the two positive charges on the metal ion. The tendency for TCNQ to dimerise means that the anions appear as dimers, i.e. $[TCNQ]_2^{2-}$. The exception to this behaviour is $[Fe(phen)_3](TCNQ)_2$ where the π interaction between the radical anions is so strong that a σ-carbon−carbon bond is formed. The formation of this σ-dianion (TCNQ−TCNQ) has previously been observed only in a few cases.[27−31]

In the reaction with $(NEt_3H)(TCNQ)_2$, with both neutral and anionic TCNQ present, the derivatives obtained correspond to the formulae $[M(terpy)_2](TCNQ)_3$ (M = Ni **4**; Cu **5**; Zn **6**) or $[M(phen)_3](TCNQ)_4$ (M = Fe **9**; Ni **10**). The TCNQ species in these compounds show an average formal charge of 0.66 e^- and 0.5 e^-, respectively, suggesting some degree of electronic delocalisation, a fact that is usually reflected in the formation of 1D TCNQ chains resulting from overlap of the π clouds of adjacent units.[11,12,32−38]

The new compounds are only slightly soluble in polar solvents such as acetonitrile or dimethyl sulfoxide. These solvents break any interactions between the metal cations and the TCNQ units which could be present in the solid state. For this reason, the solutions behave as a mixture of the metallocations and TCNQ, either in anionic or in neutral form. The spectroscopic and electrochemical data of these solutions do not give any additional information to that obtained for solid state samples, as previously described.[8,11,14] The spectroscopic data from solid-state samples will be commented upon below.

Crystal Structures

$[Ni(terpy)_2](TCNQ)_2$ (1)

This compound crystallises in the $P2_1/n$ space group. Figure 1 shows an ORTEP view of the molecular unit. The crystal structure can best be described as formed from alternating $[Ni(terpy)_2]^{2+}$ cations and dimeric $[TCNQ]_2^{2-}$anions. The nickel atom is hexacoordinated by the nitrogen atoms of the two terpy ligands in a *mer* arrangement which is expected for the ligand geometry. The nickel−nitrogen distances range between 1.994(1) and 2.132(1) Å with the shortest distances corresponding to the central nitrogen of each terpy ligand due to the strain imposed by the coordination.[39−41]

There are two crystallographically independent TCNQ molecules, A and B, in the asymmetric unit. The carbon−carbon bond lengths in the TCNQ rings are characteristic of the fully reduced radical-anion.[42] This is expected since the two positive charges in the metallic cation must be neutralised. Every $TCNQ_A$ overlaps with a $TCNQ_B$ in the ring-over-ring mode, thereby forming

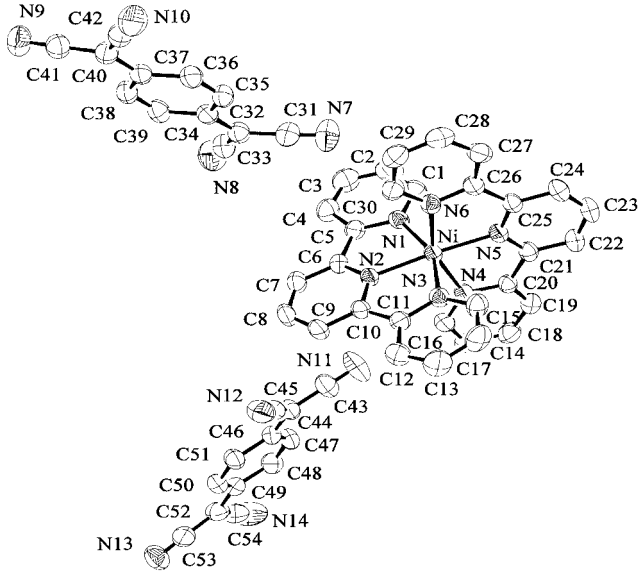

Figure 1. ORTEP view and labelling scheme of $[Ni(terpy)_2](TCNQ)_2$ (**1**); the atom labelling of the copper compound (**2**) is identical

$[TCNQ]_2^{2-}$ dianions with the shortest interplanar distance being 3.28(1) Å. The TCNQ planes are parallel to within 1.38(6)°. These planes form an angle of 31.32(6)° with one of the terpy ligands but no short contacts (less than 3.4 Å) could be found, suggesting that the cations and anions only interact by electrostatic forces in the crystal (Figure 2).

$[Cu(terpy)_2](TCNQ)_2$ (2)

This compound crystallises in the $P2_1/c$ space group. Its labelling scheme is identical to that shown in Figure 1 for the nickel derivative.

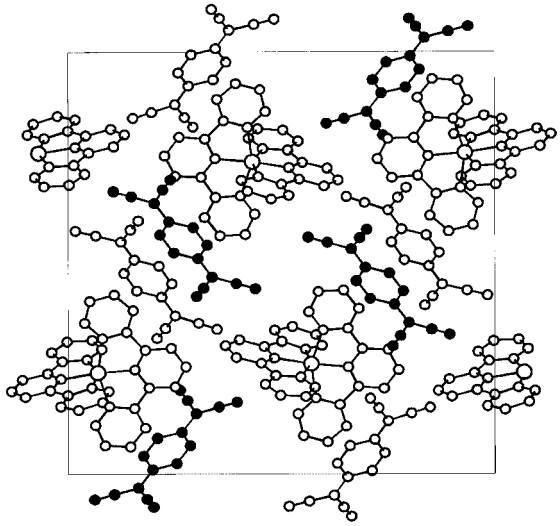

Figure 2. Unit cell contents for $[Ni(terpy)_2](TCNQ)_2$ (**1**); atoms in TCNQ A are shown as white circles and in TCNQ B as black circles

The metal environment is similar to that of the nickel derivative but the Cu−N distances vary more due to the Jahn−Teller effect which is expected for the copper centre.

This induces a rhombic distortion with opposite distances of 1.956(6) and 2.016(7) Å for the central nitrogen atoms, 2.103(6) and 2.137(7) Å for one pair of extreme nitrogen atoms and 2.250(7) and 2.277(7) Å for the other pair. A similar distortion has been observed in the structure of the parent nitrate and in related derivatives.[43−45] In accordance with these data the EPR spectrum of this compound at room temperature shows a rhombic pattern with *g* values of 2.20, 2.12 and 2.02.

There are also two crystallographically independent TCNQ anions in the cell, namely A and B, but in contrast with the nickel derivative each TCNQ overlaps with a symmetry related anion giving rise to two different $[TCNQ_A]_2^{2-}$ dimers with a ring-over-external bond overlap and a shortest interplanar distance of 3.14(1) Å and a $[TCNQ_B]_2^{2-}$ dianion overlapping in the ring-over-ring mode with a shortest distance of 3.19(1) Å (Figure 3).

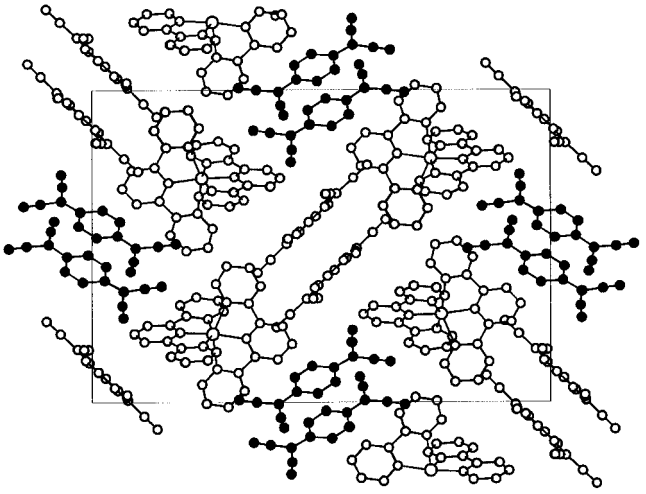

Figure 3. Unit cell contents for $[Cu(terpy)_2](TCNQ)_2$ (**2**); atoms in TCNQ A are shown as white circles and in TCNQ B as black circles

The $TCNQ_A$ dimers are isolated from the $[Cu(terpy)_2]^{2+}$ cations although the $TCNQ_B$ centres do overlap with the terpy rings of different cations through their external bonds (Figure 4) with shortest distances of 3.29(1) and 3.31(1) Å. The angle formed between the terpy and the $TCNQ_B$ is 28.0(2)°. These overlaps allow a small degree of electronic delocalisation along the tetrameric terpy·$TCNQ_B$·$TCNQ_B$·terpy stack. The stack does not continue through the solid, thus limiting possible delocalisation.

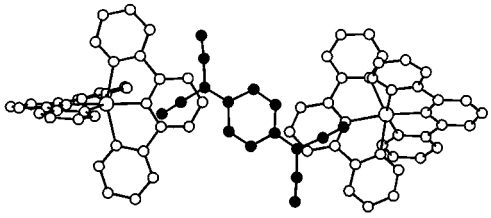

Figure 4. View of the overlap between $TCNQ_B$ and the terpy ligands of two adjacent $[Cu(terpy)_2]$ cations

[Fe(phen)$_3$](TCNQ−TCNQ) (7)

This compound crystallises in the *Cc* space group. Figure 5 shows the molecular unit with the labelling scheme. The structure can be described as formed from alternating sheets of $[Fe(phen)_3]^{2+}$ cations and σ-dimerised $[TCNQ-TCNQ]^{2-}$ anions. In the cations, the iron atom is hexacoordinated by the nitrogen atoms of three phen ligands with iron-nitrogen distances between 1.95 and 2.01 Å which is in the range usually found in other iron−phen derivatives.[46,47] The dimerised anion is obtained through the formation of a long bond between two exocyclic carbons. The carbon−carbon distance of 1.645(7) Å is similar to that found in the few cases in which this σ dimerization has been observed.[27−31] The formation of this bond is reflected in the tetrahedral conformation adopted by the linked carbon atoms, with angles between the ring plane

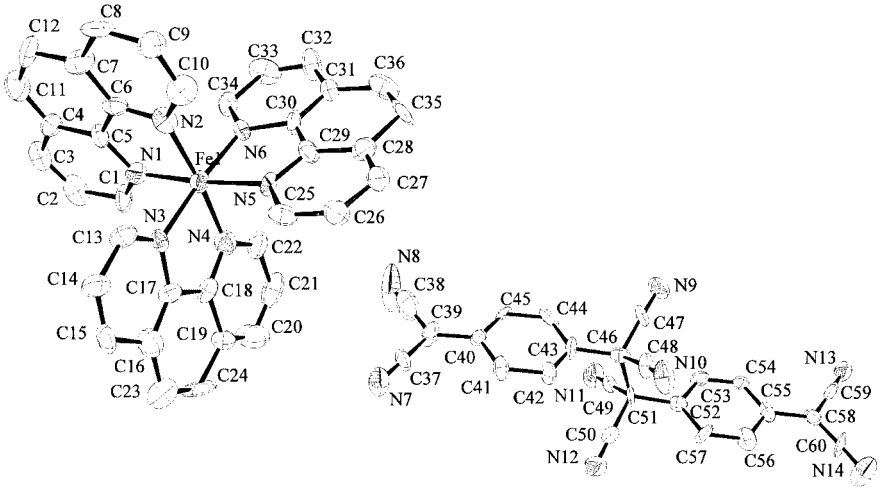

Figure 5. ORTEP view and labelling scheme of $[Fe(phen)_3](TCNQ)_2$ (**7**)

and the $C(CN)_2$ plane of 49.4(7) and 46.4(7)°, while the rest of the molecule is essentially planar.

The anions and cations are packed (Figure 6) in alternating sheets parallel to the *ab* plane and no interactions other than the usual van der Waals contacts can be found between them. Inside the anionic sheets the [TCNQ−TCNQ] units are arranged in chains along the [−1 1 0] direction with shortest contacts of 3.37(2) Å between C45 and C56.

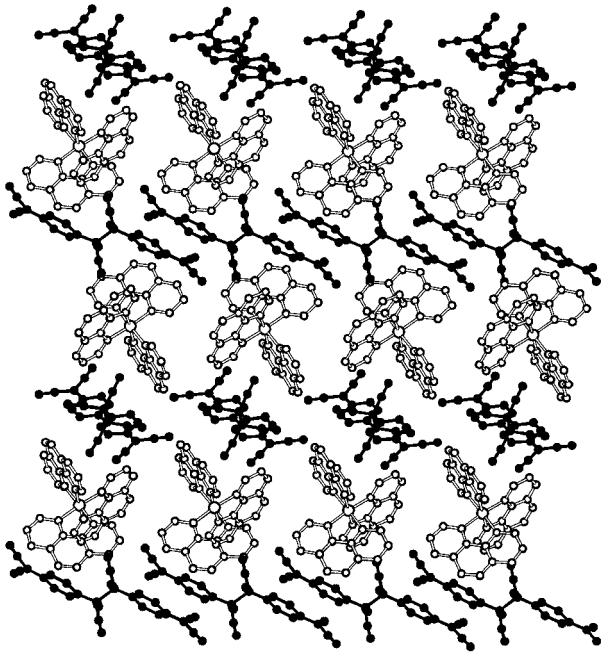

Figure 6. View of the alternating sheets of $[Fe(phen)_3]^{2+}$ cations and $[TCNQ-TCNQ]^{2-}$ anions in the structure of **7**

Spectroscopic Studies

The IR spectra of the studied derivatives show the typical features found in other uncoordinated TCNQ compounds.[48−50] The most significant bands for the neutral TCNQ are ν(CN) = 2228 cm^{-1}, $\nu_{20}(b_{1u})$ = 1530 cm^{-1} and $\nu_{50}(b_{3u})$ = 860 cm^{-1}. These bands are shifted to lower frequencies on increasing the electronic charge on the TCNQ.

The derivatives with two TCNQ units per metal atom, **1**−**3** and **8**, show these bands with typical values for the uncoordinated anion-radical, in accord with the localised picture of dimeric $[TCNQ]_2^{2-}$ anions alternating with cationic $[MN_6]^{2+}$ units in the solid structure, as the crystal structure of **1** and **2** revealed.

The spectrum of **7** shows different features attributable to the formation of a TCNQ−TCNQ σ bond. Thus, in the ν(CN) region there are two bands, the first appears at 2172 cm^{-1} and is composed of several component bands as a consequence of the lowering of the symmetry imposed by the bond formation. The second band, however, appears at 2125 cm^{-1}, a value shifted to lower frequency compared with those usually found in the anion radical. The out of plane bending mode ν_{50} also appears at 805 cm^{-1} and has been suggested as characteristic of the presence of the σ dimer,[30] since the usual value for the monoanionic species is 825 cm^{-1}.

The derivatives with three or four TCNQ units per metal atom always have the organic acceptor partially reduced, forming stacks with some degree of electronic delocalisation. This fact is reflected in the IR spectra of these species whose main feature is the presence of the tail of a low energy electronic absorption (CT_2) with broad vibrational bands superimposed on it.[51−53] The frequency values, especially the ν_{50} band, are intermediate between the usual values of the neutral and monoanionic TCNQ, suggesting that the acceptor has a formally nonintegral oxidation state. The low energy electronic transition (CT_2) appears in our compounds in the 3500−5000 cm^{-1} region and can be attributed to a charge transfer between adjacent radical anionic and neutral TCNQ groups, the lower the value the higher the electronic delocalisation.

As a consequence of this delocalisation, these compounds show semiconducting behaviour with relatively high values of electrical conductivity at room temperature and low activation energies which can be correlated with the frequency of the CT_2 electronic charge transfer as can be seen in Table 1. The activation energy was obtained by always assuming an Arrhenius dependence of the conductivity on temperature.

As expected, the derivatives with two TCNQ molecules per formula unit have localised electronic charges leading to very low conductivity values. The terpy derivatives with three TCNQ groups are much better semiconducting species. This fact can be explained if we attribute, to these compounds, a solid-state structure consisting of infinite stacks of TCNQ units separated by rows of $[M(terpy)_2]^{2+}$ cations. Every acceptor molecule in the stack would bear a negative charge of 0.66 giving rise to the formation of overlapping $[TCNQ]_3^{2-}$ trimers with partial electronic delocalisation. This structure has been previously observed in related derivatives exhibiting similar properties but with three TCNQ groups per metal atom.[11,12]

Table 1. Electronic spectra and electrical conductivity data of some representative compounds

Compound	CT_2 [cm^{-1}]	σ [S cm^{-1}] (298 K)	E_a [eV]
$[Ni(terpy)_2](TCNQ)_2$ (**1**)		$1.1\ 10^{-10}$	1.12
$[Ni(terpy)_2](TCNQ)_3$ (**4**)	3754	$1.9\ 10^{-2}$	0.25
$[Zn(terpy)_2](TCNQ)_3$ (**6**)	4378	$3.6\ 10^{-3}$	0.38
$[Ni(phen)_3](TCNQ)_4{\cdot}2CH_3CN$ (**10**)	4630	$1.8\ 10^{-4}$	0.41

The derivatives with four TCNQ groups per metal atom also show electronic delocalisation since the formal charge on every acceptor is 0.5. The reported structures of derivatives consisting of $TCNQ^{0.5-}$ show these anions stacked in nonuniform columns either forming dimerised ($[TCNQ]_2^{-}$)[38,54] or tetramerised ($[TCNQ]_4^{2-}$)[33,34,36,55] units. Both pictures correspond to a semiconductor and could suggest, for our derivatives **9**−**10**, a similar structure in the solid state.

Magnetic Properties

The bulk magnetic susceptibilities of the new compounds have been measured in the temperature range 2−300 K.

The magnetic moments of the nickel derivatives **1** and **4** follow the Curie law above 25 K with an abrupt descent in their values below this temperature as is shown for the former in Figure 7. This fact can be attributed to an anisotropic distortion of the nickel(II) environment which results in a zero field splitting of the ground state.[56] Equation (1) for the average magnetic susceptibility takes into account this single-ion anisotropy, where g_{Ni} is the Landé g factor for the nickel ion, k_B is Boltzmann's constant, β is the Bohr magneton, $x = D/k_BT$ with the parameter D measuring the zero-field splitting and $N\alpha$ is the temperature-independent paramagnetism.

$$<\chi>=(2Ng_{Ni}^2\beta^2/3k_BT)\{[2-2\exp(-x)]/x+\exp(-x)\}/[1+2\exp(-x)]+N\alpha \qquad (1)$$

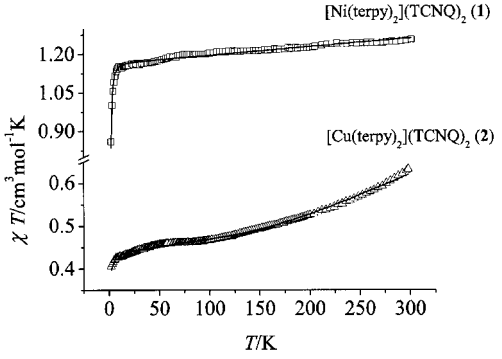

Figure 7. Temperature dependence of χT for **1** and **2**; the solid lines represent the best fit using the equations described in the text

The best fit was obtained when $g_{Ni} = 2.156$, $D = 3.34$ cm^{-1} and $N\alpha = 3.3\times10^{-4}$ cm^3mol^{-1} for **1,** and 2.07, 3.87 cm^{-1} and 9×10^{-5} cm^3mol^{-1}, respectively, for **4**. In both cases the values are typical of slightly distorted octahedral nickel(II) environments with no contribution to the magnetic moment from the organic radical anions. This is consistent with the presence of the dimerised anion-radical. The formation of dimeric $[TCNQ]_2^{2-}$ implies a strong antiferromagnetic coupling of both spins which renders the dianion diamagnetic at room temperature. The magnetic susceptibility variation can then be exclusively attributed to the contribution of the isolated metal ion. In accord with this behaviour, the zinc derivatives **3** and **6** are diamagnetic since no magnetic contribution can be expected from the metal ion.

The copper derivative **2** shows a steady increase in its χT value on increasing the temperature (Figure 7). The small decrease in the value at low temperatures can be ascribed to very weak antiferromagnetic interactions between the almost isolated copper(II) centres and can be fitted with the Curie−Weiss law. The increase in the χT value above 125 K is due to a small contribution from the TCNQ dimers which show a lower antiferromagnetic coupling than exhibited by the nickel and zinc derivatives. The lower value of the coupling implies that the triplet state is thermally accessible and populated near room temperature, giving rise to the contribution from the radicals to the magnetic susceptibility. Taking these two contributions into account, the molar magnetic susceptibility was fit, using Equation (2), to the sum of the Curie−Weiss law for the copper(II) ion and the Bleaney−Bowers equation[57] for the antiferromagnetically interacting TCNQ radicals, where g_{Cu} is the Landé g factor for the copper ion, J is the exchanging coupling constant for the TCNQ dimers, g is the Landé g factor for the TCNQ radicals and is assumed to be 2.003.

$$\chi=\frac{Ng_{Cu}^2\beta^2}{4k_B(T-\theta)}+\frac{Ng^2\beta^2}{k_BT}\left[\frac{2}{3+\exp(-J/k_BT)}\right]+N\alpha \qquad (2)$$

The rest of the parameters are the same as in Equation (1). The best fit for the experimental data, represented as a solid line in Figure 7, corresponds to $g_{Cu} = 2.161$, $\theta = -0.21$ K, $J = -278$ cm^{-1} and $N\alpha = 3.2\times10^{-4}$ cm^3mol^{-1}.

In contrast, compound **5** does not show any contribution from the organic radicals to the magnetic susceptibility which can be fit to the sum of the Curie−Weiss contribution from the copper ion, the first term in Equation (2) and the temperature-independent paramagnetism. The values obtained are $g_{Cu} = 2.26$, $\theta = -0.9$ K and $N\alpha = 8.4\times10^{-4}$ cm^3mol^{-1}. The high value of the TIP compared with those of the other compounds can probably be attributed to an incomplete diamagnetic correction although it is also plausible that it is due to a Pauli contribution originating from the delocalised electron of the anion radicals since the value is in the range of the paramagnetism observed in other conducting radical salts.[12,58] On the other hand, the low θ value for both copper derivatives indicates that the exchange between neighbouring copper spins can be considered negligible.

The phen derivatives show different behaviour, especially those showing electronic delocalisation. The iron derivative **7** is diamagnetic and corresponds to the presence of a low spin iron(II) and coupling between the two electrons with the formation of a TCNQ−TCNQ σ-bond. The magnetic susceptibility of the nickel derivative **8** is characteristic of isolated S = 1 spins and can be fitted to Equation (1) with values of $g_{Ni} = 1.94$, $D = 1.28$ cm^{-1} and $N_\alpha = 10^{-4}$ cm^3mol^{-1}.

The magnetic susceptibilities of the derivatives **9** and **10**, with four TCNQ units per metal atom, show the contribution of the organic radicals which only partially couple in an antiferromagnetic manner.

The iron derivative **9** is weakly paramagnetic and this paramagnetism can only be attributed to the organic radicals since the low spin iron(II) has no unpaired electrons. The susceptibility dependence with temperature (Figure 8) can be interpreted as the sum of three contributions: (i) the contribution of the spins located on the TCNQ which can be adjusted to a 1D antiferromagnetic chain of S = 1/2 spins and which is responsible for the maximum around 65 K, (ii) a Curie contribution from a paramagnetic impurity which may arise from isolated radicals in the structure which gives the increase in susceptibility at lower temperatures and (iii) temperature-independent paramagnetism. The first contribution has been fit with a Heisenberg linear chain model using the expression derived by Hatfield et al.[59] and constitutes the first term of Equation (3) where $x = |J|/k_BT$ and A, B, C, D, E and F are functions of α, a parameter that takes into account the distortion in the chain and can vary from $\alpha = 0$ (corresponding to isolated $TCNQ^-$ dimers) to $\alpha = 1$ (corresponding to a uniform chain of S = 1/2 spins). The second term of Equation (3) is the Curie contribution from the impurities with C being the Curie constant, while the final term is the TIP. The other parameters have the same meaning as in Equations (1) and (2).

$$\chi = \frac{Ng^2\beta^2}{k_BT}\left[\frac{A+Bx+Cx^2}{1+Dx+Ex^2+Fx^3}\right]+\frac{C}{T}+N\alpha \quad (3)$$

The best fit has been obtained assuming $g = 2.003$ for the TCNQ group and affords $J = -44$ cm^{-1}, $\alpha = 0.67$, $C = 0.007$ cm^{3}mol^{-1}K and $N\alpha = 1.5\times10^{-4}$ cm^{3}mol^{-1}. These parameters indicate the presence of a 2% of paramagnetic impurity and that the TCNQ units are probably stacked into infinite chains. The low values of the exchange constant and the α parameter suggest that these molecules can form dimeric $[TCNQ]_2^-$ units with poorer π overlap between adjacent dimers than can be found inside the dimer. Similar behaviour was found in [Fe(cyclam)(NCS)$_2$](TCNQ)$_2$ [38] with a similar J value (-43 cm^{-1}) but with a more uniform stack reflected in a higher α value (0.85) and also in [Zn(phen)$_3$](TCNQ)$_2$[5] which shows only half of the TCNQ anions stacked in an alternating chain ($J = -41$ cm^{-1}, $\alpha = 0.8$).

The nickel derivative **10** shows different magnetic behaviour. The general variation of χT (Figure 9) shows typical values for a nickel(II) ion in the 15−50 K range with a pronounced decrease at low temperatures which can be interpreted in terms of the zero-field splitting induced by the anisotropy in the nickel environment and an increase in χT values at higher temperatures, attributable to the contribution of the stacked TCNQ units. The data below 50 K were then fit to Equation (1) affording the values $g_{Ni} = 2.139$, $D = 1.54$ cm^{-1} and $N\alpha = 2.1\times10^{-4}$ cm^{3}mol^{-1}, while the data above 50 K were treated as consisting of three contributions: that of the nickel ion, the contribution from the antiferromagnetically interacting TCNQ radicals and the temperature-independent paramagnetism [Equation (4)]. In this temperature range we have ignored the contribution from the nickel zero field splitting since the low value previously found can be considered negligible. For this reason the nickel contribution is simply that obtained by the Curie law. The TCNQ groups have been assumed to be showing behaviour similar to that found in the iron derivative and their contribution has therefore been fit to a Heisenberg linear chain model where χ_{TCNQ} corresponds to the first term of Equation (3).

$$\chi = \frac{2Ng_{Ni}^2\beta^2}{3k_BT}+\chi_{TCNQ}+N\alpha \quad (4)$$

The best fit, shown in Figure 9 as a solid line, affords the following values $g_{Ni} = 2.14$, $J = -103$ cm^{-1}, $\alpha = 0.36$ and $N\alpha = 5\times10^{-4}$ cm^{3}mol^{-1}. The picture given by these data suggests an even less uniform chain in this compound which shows pairs of S = 1/2 spins coupling strongly in an antiferromagnetic way with weaker coupling between adjacent pairs. However, the lack of crystal structures precludes closer conclusions being drawn between the nonuniform 1D TCNQ stack deduced from magnetic observations and the actual structure in the solid state.

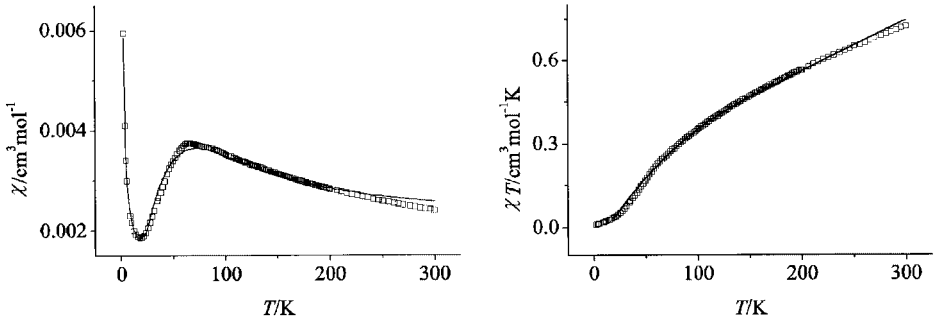

Figure 8. Plots of the magnetic susceptibility (left) and χT (right) of **9** as a function of the temperature; the solid line corresponds to the fit of the experimental data

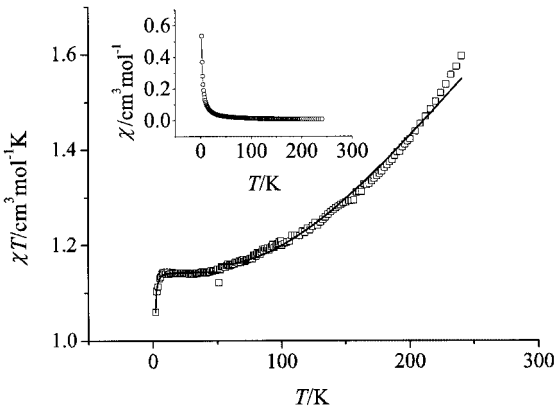

Figure 9. Plot of χT for **10** as a function of the temperature; the solid line corresponds to the fit of the experimental data; the inset shows the magnetic susceptibility plot of this compound

Concluding Remarks

The formation TCNQ derivatives with different stoichiometries can be seen as the result of the combination of two factors, namely the electrostatic interaction resulting from the neutralisation of the positive charges in the metallic fragment by the $TCNQ^-$ anion-radicals and the steric requirements that the cationic fragment imposes.[36] In derivatives having only monoanionic TCNQ, namely $[M(terpy)_2](TCNQ)_2$ and $[M(phen)_3](TCNQ)_2$, the tendency of the anion-radical to dimerise gives rise to the formation of S = 0 dianions $[TCNQ]_2^{2-}$. Since the metal coordination environment is saturated, no direct interaction with the TCNQ can be observed and the packing of metal cations surrounded by dimeric dianions is the structural motif which describes the solid state arrangement. This is also true when the strong interaction between adjacent TCNQ gives rise to the formation of a σ-bonded dimer in $[Fe(phen)_3](TCNQ)_2$. The strong coupling inside the $[TCNQ]_2^{2-}$ dimer leads to a diamagnetic state for the organic acceptors which do not contribute to the magnetic susceptibility. The exception is $[Cu(terpy)_2](TCNQ)_2$, for which the dimer excited triplet state becomes thermally accessible. This fact can be attributed to a weakening in the antiferromagnetic intradimer coupling as a consequence of the π interactions between $TCNQ^-$ and the aromatic ring of one terpy ligand found in the crystal structure of this compound. This is not observed in the analogous nickel derivative. In previous reports, the isolated $[TCNQ]_2^{2-}$ never contributes to the magnetic susceptibility[8,12,13,50] but when the dimers overlap with adjacent π systems, a weaker coupling can be observed.[11,50,55,60] In the previous cases, the dimeric dianion overlapped with a more or less neutral TCNQ but the unprecedented situation in this complex is that this role is assumed by one of the aromatic rings of the ligand.

In the derivatives with TCNQ in nonintegral oxidation states two compositions have been found, namely $[M(terpy)_2](TCNQ)_3$ and $[M(phen)_3](TCNQ)_4$. The magnetic properties of these derivatives are in accordance with the presence of 1D stacks of either trimeric $[TCNQ]_3^{2-}$ or tetrameric $[TCNQ]_4^{2-}$ units. Thus, in derivatives with $TCNQ^{0.66-}$, no contribution from the organic acceptor is usually observed,[12] whereas with stacked $TCNQ^{0.5-}$ units, linear chain magnetic behaviour from the organic part has been proposed.[38,61] The different stoichiometry for these derivatives can be explained in terms of the size of the metal cation and on the basis that only electrostatic interactions can occur between the cationic units and the negative TCNQ stacks. Assuming that the cations behave as rigid spheres which do not interpenetrate, we can estimate the diameter of the $[M(terpy)_2]^{2+}$ unit as ca. 11.3 Å, i.e. as measured in **1** (in fact the measured nickel-nickel distance of 11.8 Å matches well with this assumption), while a diameter for the $[M(phen)_3]^{2+}$ unit of ca. 13.4 Å has been estimated from the crystal structure of **7**. The TCNQ stack must then accommodate the three or four TCNQ units, bearing the two negative charges, in the same space occupied by the counterion. Since the stacking distances between adjacent TCNQ units appear in the 3.10−3.25 Å range, three TCNQ units will occupy 9.3−9.75 Å, while four TCNQ units need 12.4−13.0 Å in the stack. According to this picture, three TCNQ derivatives will form next to a dipositive cation of less than ca. 12 Å in diameter whereas the four TCNQ unit derivative must be obtained with bigger cations.

Experimental Section

General Remarks: All reactions were carried out under oxygen-free nitrogen. The parent reagents $[M(terpy)_2](NO_3)_2$,[43,62] $[M(phen)_3](NO_3)_2$,[63] LiTCNQ[64] and $(NEt_3H)(TCNQ)_2$ [64] were obtained by the published methods and their purities were checked by elemental analysis. Elemental analyses were carried out by the Servicio de Microanálisis of the Universidad Complutense de Madrid. Infrared spectra were recorded as KBr pellets with a Nicolet Magna-550 FT-IR spectrophotometer. Electronic spectra were recorded using a Cary-5 spectrophotometer. The spectra were recorded either in solution or in the solid state. The solid samples were prepared by rubbing the sample on optical glass. Magnetic experiments were carried out on polycrystalline samples using a SQUID magnetometer MPMS-XL-5 manufactured by Quantum Design. The temperature dependence of the magnetisation in the range between 2 and 300 K was recorded using a constant magnetic field of 0.5 T. The experimental data were corrected for the magnetisation of the sample holder and for atomic diamagnetism as calculated from Pascal's constants. Electrical conductivity data were measured by the two points method on single crystals using an APD cryogenics INC HC2 helium cryostat.

Preparation of the $[M(terpy)_2](TCNQ)_2$ Derivatives: All compounds of this type were obtained by the same procedure. A solution containing LiTCNQ (0.15 mmol) in methanol (15 mL) was added dropwise to a solution of the starting nitrate (0.075 mmol) in a mixture of methanol (15 mL)/water (5 mL). After complete mixing a blue solid appeared which was filtered, washed with methanol and dried under vacuum.

$[Ni(terpy)_2](TCNQ)_2$ (1): Yield 45 mg, 64%. $C_{54}H_{30}N_{14}Ni$ (933.6): calcd. C 69.5, H 3.2, N 21.0; found C 69.6, H 3.2, N 20.9. IR

(KBr): $\tilde{\nu}$ = 2183 s, 2176 s, 2155 s, 1584 m, 1504 m, 1473 m, 1450 w, 1350 m, 1177 m, 987 w, 830 w, 820 w, 772 m cm^{-1}.

[Cu(terpy)$_2$](TCNQ)$_2$ (2): Yield 50 mg, 71%. $C_{54}H_{30}CuN_{14}$ (938.5): calcd. C 69.1, H 3.2, N 20.9; found C 68.8, H 3.4, N 21.1. IR (KBr): $\tilde{\nu}$ = 2183 s, 2174 s, 2157 s, 1583 m, 1505 m, 1474 m, 1450 w, 1363 m, 1175 m, 987 w, 824 w, 770 m cm^{-1}.

[Zn(terpy)$_2$](TCNQ)$_2$ (3): Yield 47 mg, 67%. $C_{54}H_{30}N_{14}Zn$ (940.3): calcd. C 69.0, H 3.2, N 20.8; found C 68.4, H 3.3, N 20.5. IR (KBr): $\tilde{\nu}$ = 2184 s, 2174 s, 2151 s, 1583 m, 1506 m, 1475 m, 1452 w, 1358 m, 1182 m, 988 w, 828 w, 772 m cm^{-1}.

Preparation of the [M(terpy)$_2$](TCNQ)$_3$ Derivatives: A solution containing $(NEt_3H)(TCNQ)_2$ (0.13 mmol) in acetonitrile (20 mL) was added dropwise to a solution of the starting nitrate (0.065 mmol) in a mixture of methanol (15 mL)/water (5 mL). After complete mixing a dark blue solid appeared which was filtered, washed with methanol and dried under vacuum.

[Ni(terpy)$_2$](TCNQ)$_3$ (4): Yield 46 mg, 62%. $C_{66}H_{34}N_{18}Ni$ (1137.8): calcd. C 69.7, H 3.0, N 22.2; found C 69.6, H 3.1, N 22.3. IR (KBr): $\tilde{\nu}$ = 2200 m, 2186 s, 2175 s, 2155 s, 1572 m, 1505 m, 1472 m, 1449 w, 1357 m, 1159 m, 983 w, 833 w, 826 w, 773 m cm^{-1}.

[Cu(terpy)$_2$](TCNQ)$_3$ (5): Yield 49 mg, 66%. $C_{66}H_{34}CuN_{18}$ (1142.7): calcd. C 69.4, H 3.0, N 22.1; found C 69.5, H 3.0, N 21.9. IR (KBr): $\tilde{\nu}$ = 2196 s, 2168 s, 2155 s, 1570 m, 1508 m, 1476 m, 1451 w, 1352 m, 1330 m, 1182 m, 990 w, 837 w, 826 w, 773 m cm^{-1}.

[Zn(terpy)$_2$](TCNQ)$_3$ (6): Yield 43 mg, 58%. $C_{66}H_{34}N_{18}Zn$ (1144.5): calcd. C 69.3, H 3.0, N 22.0; found C 68.7, H 3.1, N 21.7. IR (KBr): $\tilde{\nu}$ = 2194 s, 2168 s, 2155 s, 1564 m, 1506 m, 1476 m, 1454 w, 1361 m, 1323 m, 1134 m, 985 w, 832 w, 773 m cm^{-1}.

Preparation of the [M(phen)$_3$](TCNQ)$_2$ Derivatives: A solution containing LiTCNQ (0.2 mmol) in methanol (15 mL) was added dropwise to a solution of the starting nitrate (0.1 mmol) in a methanol/water (15 mL + 5 mL) mixture. After complete mixing, a blue solid appeared which was filtered, washed with methanol and dried under vacuum.

[Fe(phen)$_3$](TCNQ)$_2$ 2CH$_3$OH (7): Yield 68 mg, 64%. $C_{62}H_{40}FeN_{14}O_2$ (1068.9): calcd. C 69.7, H 3.8, N 18.3; found C 69.3, H 3.7, N 18.1. IR (KBr): $\tilde{\nu}$ = 2179 s, 2125 s, 1600 s, 1580 m, 1503 s, 1330 m, 1179 m, 846 m, 804 w, 723 m cm^{-1}.

[Ni(phen)$_3$](TCNQ)$_2$ (8): Yield 69 mg, 69%. $C_{60}H_{32}N_{14}Ni$ (1007.7): calcd. C 71.5, H 3.2, N 19.4; found C 70.8, H 3.3, N 19.2. IR (KBr): $\tilde{\nu}$ = 2177 s, 2152 s, 1585 m, 1505 w, 1426 m, 1357 s, 1180 m, 987 w, 844 w, 838 w, 827 w, 726 m cm^{-1}.

Preparation of the [M(phen)$_3$](TCNQ)$_4$ Derivatives: A solution containing $(NEt_3H)(TCNQ)_2$ (1 mmol) in acetonitrile (15 mL) was added dropwise to a solution of the starting nitrate (0.5 mmol) in methanol (15 mL). After complete mixing, a dark blue solid appeared which was filtered, washed with methanol and diethyl ether and dried under vacuum.

[Fe(phen)$_3$](TCNQ)$_4$·2CH$_3$CN (9): Yield 46 mg, 61%. $C_{88}H_{46}FeN_{24}$ (1495.4): calcd. C 70.7, H 3.1, N 22.5; found C 71.3, H 3.2, N 22.0. IR (KBr): $\tilde{\nu}$ = 2200 s, 2158 s, 1558 m, 1520 w, 1506 w, 1425 m, 1320 s, 1304 s, 1096 s, 952 w, 850 w, 841 w, 721 w, 688 m cm^{-1}.

[Ni(phen)$_3$](TCNQ)$_4$·2CH$_3$CN (10): Yield 43 mg, 57%. $C_{88}H_{46}N_{24}Ni$ (1498.2): calcd. C 70.5, H 3.1, N 22.4; found C 70.3, H 3.2, N 22.3. IR (KBr): $\tilde{\nu}$ = 2196 w, 2169 s, 2156 s, 1558 m, 1520 m, 1505 m, 1426 m, 1328 m, 1131 m, 953 w, 845 w, 728 m, 697 m cm^{-1}.

X-ray Crystallographic Studies: Good quality crystals of **1**, **2** and **7** were obtained by slow diffusion of dilute solutions of the reactants. A summary of the fundamental crystal data is given in Table 2. The crystal data were collected at the "CAI de Difracción de Rayos X, UCM". In each of the three cases, a deep blue crystal was co-

Table 2. Crystal and refinement data for [Ni(terpy)$_2$](TCNQ)$_2$ (**1**), [Cu(terpy)$_2$](TCNQ)$_2$ (**2**) and [Fe(phen)$_3$](TCNQ)$_2$·2CH$_3$OH (**7**)

	1	**2**	**7**
Empirical formula	$C_{54}H_{30}N_{14}Ni$	$C_{54}H_{30}CuN_{14}$	$C_{62}H_{40}FeN_{14}O_2$
Formula mass	933.63	938.46	1068.93
Crystal system	monoclinic	monoclinic	monoclinic
Space group	$P2_1/n$ (No. 14)	$P2_1/c$ (No. 14)	Cc (No. 9)
a [Å]	8.653(2)	8.858(1)	12.856(1)
b [Å]	22.828(5)	18.569(1)	14.955(1)
c [Å]	23.779(5)	27.463(1)	25.999(3)
α [°]	90	90	90
β [°]	93.16(3)	94.51(1)	91.718(2)
γ [°]	90	90	90
Z	4	4	4
V [Å^3]	4690(1)	4503.4(6)	4996.3(8)
$D_{calcd.}$ [Mg·m^{-3}]	1.322	1.384	1.422
μ [mm^{-1}]	0.468	0.541	0.366
θ range [°]	1.72−30.55	1.49−22.97	1.57−28.74
Reflections collected	53215	5096	9448
Independent reflections	13777	4975	5591
Refined parameters	622	622	716
Goodness of fit	0.893	0.920	0.604
Absolute structure parameter	−	−	0.05(5)
$R1$[a] [$I > 2\sigma(I)$]	0.0416	0.0496	0.0423
$wR2$[b] [$I > 2\sigma(I)$]	0.0892	0.0863	0.1084

[a] $R1 = \Sigma(|F_o| - |F_c|)^2/\Sigma F_o^2$. [b] $wR2 = \{\Sigma[w(F_o^2 - F_c^2)^2]/\Sigma[w(F_o^2)^2]\}^{1/2}$.

ated with resin epoxy and mounted on a Bruker Smart CCD diffractometer using graphite-monochromated Mo-K_α radiation (λ = 0.71073 Å) operating at 50 kV and 25A. Data were collected over a reciprocal space hemisphere by combination of three exposure sets. Each frame exposure time was 20 s covering 0.3° in ω. The cell parameters were determined and refined by least-squares fits of all reflections collected. The first 50 frames were recollected at the end of the data collection to monitor crystal decay but no appreciable decay was observed. The structures were solved by direct and Fourier methods and refined by applying full-matrix least squares on F^2 with anisotropic thermal parameters for the non-hydrogen atoms. The hydrogen atoms were included with fixed isotropic contributions in their calculated positions determined by molecular geometry. The calculations were carried out with the SHELX97 software package.[65] CCDC-238898 (**1**), -238899 (**2**) and -238900 (**7**) contain the supplementary crystallographic data for this paper. These data can be obtained free of charge at www.ccdc.cam.ac.uk/conts/retrieving.html (or from the Cambridge Crystallographic Data Centre, 12 Union Road, Cambridge CB2 1EZ, UK; Fax: (internat.) + 44-1223-336-033; E-mail: deposit@ccdc.cam.ac.uk).

Acknowledgments

We gratefully acknowledge the Spanish Ministerio de Ciencia y Tecnología, project BQU2002-01409, for financial support.

[1] M. Kurmoo, A. W. Graham, P. Day, S. J. Coles, M. B. Hursthouse, J. L. Caulfield, J. Singleton, F. L. Pratt, W. Hayes, L. Ducasse, P. Guionneau, *J. Am. Chem. Soc.* **1995**, *117*, 12209.
[2] C. Chen, K. S. Suslick, *Coord. Chem. Rev.* **1993**, *128*, 293.
[3] W. Kaim, M. Moscherosch, *Coord. Chem. Rev.* **1994**, *129*, 157.
[4] H. Zhao, R. A. Heintz, K. R. Dunbar, R. D. Rogers, *J. Am. Chem. Soc.* **1996**, *118*, 12844.
[5] A. Bencini, S. Mindolini, C. Zanchini, *Inorg. Chem.* **1989**, *28*, 1963.
[6] J. P. Cornelissen, J. H. Diemen, L. R. Groenveld, J. G. Hasnoot, A. L. Speck, R. J. Reedijk, *Inorg. Chem.* **1992**, *31*, 198.
[7] M. C. Muñoz, J. Cano, R. Ruiz, F. Lloret, J. Faus, *Acta Crystallogr., Sect. C* **1995**, *51*, 873.
[8] L. Ballester, A. Gutiérrez, M. F. Perpiñán, U. Amador, M. T. Azcondo, A. E. Sánchez-Peláez, C. Bellitto, *Inorg. Chem.* **1997**, *36*, 6390.
[9] H. Endress, *Angew. Chem. Int. Ed. Engl.* **1982**, *21*, 524.
[10] H. Endress, *Angew. Chem. Int. Ed. Engl.* **1984**, *23*, 999.
[11] M. T. Azcondo, L. Ballester, S. Golhen, A. Gutiérrez, L. Ouahab, S. Yartsev, P. Delhaes, *J. Mater. Chem.* **1999**, *9*, 1237.
[12] L. Ballester, A. M. Gil, A. Gutiérrez, M. F. Perpiñán, M. T. Azcondo, A. E. Sánchez-Peláez, E. Coronado, C. J. Gómez-García, *Inorg. Chem.* **2000**, *39*, 2837.
[13] P. J. Kunkeler, P. J. van Koningsbruggen, J. P. Cornelissen, A. N. van der Horst, A. M. van der Kraan, A. L. Spek, J. G. Haasnoot, J. Reedijk, *J. Am. Chem. Soc.* **1996**, *118*, 2190.
[14] L. Ballester, M. C. Barral, A. Gutiérrez, A. Monge, M. F. Perpiñán, C. Ruiz-Valero, A. Sánchez-Peláez, *Inorg. Chem.* **1994**, *33*, 2142.
[15] M. T. Azcondo, L. Ballester, A. Gutiérrez, M. F. Perpiñán, U. Amador, C. Ruiz-Valero, C. Bellitto, *J. Chem. Soc., Dalton Trans.* **1996**, 3015.
[16] L. Ballester, A. Gutiérrez, M. F. Perpiñán, M. T. Azcondo, A. E. Sánchez-Peláez, U. Amador, *Anal. Quim. Int. Ed.* **1996**, *92*, 275.
[17] H. J. Keller, I. Leichert, M. Megnamisi-Belombre, D. Nothe, J. Weiss, *Z. Anorg. Allg. Chem.* **1977**, *429*, 231.
[18] N. Matsumoto, Y. Nonaka, S. Kida, S. Kawano, I. Ueda, *Inorg. Chim. Acta* **1979**, *37*, 27.
[19] P. Cassoux, A. Gleizes, *Inorg. Chem.* **1980**, *19*, 665.
[20] L. J. Pace, A. Ulman, J. A. Ibers, *Inorg. Chem.* **1982**, *21*, 199.
[21] N. Matsumoto, T. Miyazaki, Y. Sagara, A. Ohyoshi, *Inorg. Chim. Acta* **1982**, *63*, 249.
[22] M. Soriano-Garcia, R. A. Toscano, J. Gomez-Lara, M. E. Lopez-Morales, *Acta Crystallogr., Sect. C* **1985**, *41*, 1024.
[23] P. Bergamini, V. Bertolasi, V. Ferretti, S. Sostero, *Inorg. Chim. Acta* **1987**, *126*, 151.
[24] P. J. Spellane, L. V. Interrante, R. K. Kullnig, F. S. Tham, *Inorg. Chem.* **1989**, *28*, 1587.
[25] M. Shiotsuka, Y. Okaue, N. Matsumoto, H. Okawa, T. Isobe, *J. Chem. Soc., Dalton Trans.* **1994**, 2065.
[26] A. Togni, M. Hobi, G. Rihs, G. Rist, A. Albinati, P. Zanello, D. Zech, H. Keller, *Organometallics* **1994**, *13*, 1224.
[27] V. Dong, H. Endres, H. J. Keller, W. Moroni, D. Nöthe, *Acta Crystallogr., Sect. B* **1977**, *33*, 2428.
[28] B. Morosin, H. J. Plastas, L. B. Coleman, J. M. Stewart, *Acta Crystallogr., Sect. B* **1978**, *54*, 540.
[29] S. K. Hoffmann, P. J. Corvan, P. Singh, C. N. Sethulekshmi, W. E. Hatfield, *J. Am. Chem. Soc.* **1983**, *105*, 4608.
[30] H. Zhao, R. A. Heintz, X. Ouyang, K. R. Dunbar, C. F. Campana, R. D. Rogers, *Chem. Mater.* **1999**, *11*, 736.
[31] S. Mikami, K. Sugiura, J. S. Miller, Y. Sakata, *Chem. Lett.* **1999**, 413.
[32] H. Kobayashi, Y. Ohashi, F. Marumo, Y. Saito, *Acta Crystallogr., Sect. B* **1970**, *26*, 459.
[33] S. Z. Goldberg, R. Eisenberg, J. S. Millar, A. J. Epstein, *J. Am. Chem. Soc.* **1976**, *98*, 5173.
[34] A. Bosch, B. van Bodegom, *Acta Crystallogr., Sect. B* **1977**, *33*, 3013.
[35] C. P. Lau, P. Singh, S. J. Cline, R. Seiders, M. Brookhart, W. E. Marsh, D. J. Hodgson, W. E. Hatfield, *Inorg. Chem.* **1982**, *21*, 208.
[36] M. D. Ward, P. J. Fagan, J. C. Calabrese, D. C. Johnson, *J. Am. Chem. Soc.* **1989**, *111*, 1719.
[37] F. Conan, J. S. Pala, M. T. Garland, R. Baggio, *Inorg. Chim. Acta* **1998**, *278*, 108.
[38] L. Ballester, A. Gutiérrez, M. F. Perpiñán, S. Rico, M. T. Azcondo, C. Bellitto, *Inorg. Chem.* **1999**, *38*, 4430.
[39] E. N. Maslen, C. L. Raston, A. H. White, *J. Chem. Soc., Dalton Trans.* **1974**, 1803.
[40] C. L. Raston, A. H. White, *J. Chem. Soc., Dalton Trans.* **1976**, 7.
[41] A. T. Baker, D. C. Craig, A. D. Rae, *Aust. J. Chem.* **1995**, *48*, 1373.
[42] S. Flandrois, D. Chasseau, *Acta Crystallogr., Sect. B* **1977**, *33*, 2744.
[43] R. Allmann, W. Henke, D. Reinen, *Inorg. Chem.* **1978**, *17*, 378.
[44] M. I. Arriortua, T. Rojo, J. M. Amigo, G. Germain, J. P. Declercq, *Acta Crystallogr., Sect. B* **1982**, *38*, 1323.
[45] J. Valdes-Martinez, R. A. Toscazo, D. Salazar-Mendoza, *Acta Crystallogr., Sect. E* **2001**, *57*, 331.
[46] A. Zalkin, D. H. Templeton, T. Ueki, *Inorg. Chem.* **1973**, *12*, 1641.
[47] J. Baker, L. M. Engelhardt, B. N. Figgis, A. H. White, *J. Chem. Soc., Dalton Trans.* **1975**, 530.
[48] R. Bozio, A. Girlando, C. Pecile, *J. Chem. Soc., Faraday Trans.* **1975**, *71*, 1237.
[49] R. Bozio, I. Zanon, A. Girlando, C. Pecile, *J. Chem. Soc., Faraday Trans. 2* **1978**, *74*, 235.
[50] L. Ballester, A. Gutiérrez, M. F. Perpiñán, M. T. Azcondo, *Coord. Chem. Rev.* **1999**, *190−192*, 447.
[51] M. Inoue, M. B. Inoue, *J. Chem. Soc., Faraday Trans.* **1985**, *81*, 539.
[52] E. Ghezzal, A. Brau, J. P. Farges, P. Dupuis, *Mol. Cryst. Liq. Cryst.* **1992**, *211*, 327.
[53] J. B. Torrance, *Acc. Chem. Res.* **1979**, *12*, 79.
[54] C. Willi, A. H. Reis Jr., E. Gebert, J. S. Miller, *Inorg. Chem.* **1981**, *20*, 313.
[55] M. Fourmigué, V. Perrocheau, R. Clérac, C. Coulon, *J. Mater. Chem.* **1997**, *7*, 2235.

[56] R. L. Carlin, *Magnetochemistry*, Springer-Verlag, Berlin, **1986**, p. 24.
[57] B. Bleaney, K. D. Bowers, *Proc. R. Soc. London, Ser. A* **1952**, *214*, 451.
[58] J. M. Williams, J. R. Ferraro, R. J. Thorn, K. D. Carlson, U. Geiser, H. H. Wang, A. M. Kini, M. H. Whangbo in *Organic Superconductors. Synthesis, Structure, Properties and Theory* (Ed.: R. N. Grimes), Prentice Hall, Englewood Cliffs, New Jersey, USA, **1992**.
[59] J. W. Hall, W. E. Marsh, R. R. Weller, W. E. Hatfield, *Inorg. Chem.* **1981**, *20*, 1033.
[60] L. Ballester, A. Gutiérrez, M. F. Perpiñán, A. E. Sánchez, M. T. Azcondo, M. J. González, *Inorg. Chim. Acta* **2004**, *357*, 1054.
[61] S. Huizinga, G. Kommandeur, G. A. Sawatzky, B. T. Thole, L. Kopinga, W. J. M. de Jonge, J. Ros, *Phys. Rev. B* **1979**, *19*, 4723.
[62] S. Kremer, W. Henke, D. Reinen, *Inorg. Chem.* **1982**, *21*, 3013.
[63] R. G. Inskeep, *J. Inorg. Nucl. Chem.* **1962**, *24*, 763.
[64] L. R. Melby, R. J. Herder, W. Mahler, R. E. Benson, W. E. Mochel, *J. Am. Chem. Soc.* **1962**, *84*, 3374.
[65] G. M. Sheldrick, *SHELX-97*, University of Göttingen, Germany, **1997**.

Received June 18, 2004
Early View Article
Published Online December 13, 2004

